

CERN-TH/98-294  
hep-ph/9810370

# Vector-Meson Electroproduction from Generalized Vector Dominance

Dieter Schildknecht<sup>a</sup>

Theoretical Physics Division, CERN, CH-1211 Geneva 23  
and

Fakultät für Physik, Universität Bielefeld, D-33501 Bielefeld

Gerhard A. Schuler<sup>b</sup>

Theoretical Physics Division, CERN, CH-1211 Geneva 23

and

Bernd Surrow

Experimental Physics Division, CERN, CH-1211 Geneva 23

## Abstract

Including destructively interfering off-diagonal transitions of diffraction-dissociation type, we arrive at a formulation of GVD for exclusive vector-meson production in terms of a continuous spectral representation of dipole form. The transverse cross-section,  $\sigma_{T,\gamma^*p \rightarrow Vp}$ , behaves asymptotically as  $1/Q^4$ , while  $R_V \equiv \sigma_{L,\gamma^*p \rightarrow Vp}/\sigma_{T,\gamma^*p \rightarrow Vp}$  becomes asymptotically constant. Contributions violating  $s$ -channel helicity conservation stay at the 10–15% level established in low-energy photoproduction and diffractive hadron–hadron interactions. The data for  $\phi$ - and  $\rho^0$ -meson production for  $0 \lesssim Q^2 \lesssim 20 \text{ GeV}^2$  from HERA are found to be in agreement with these predictions.

CERN-TH/98-294  
September 1998

---

<sup>a</sup> Supported by the BMBF, Bonn, Germany, Contract 05 7BI92P and the EC-network contract CHRX-CT94-0579.

<sup>b</sup> Heisenberg Fellow; supported in part by the EU Fourth Framework Programme “Training and Mobility of Researchers”, Network “Quantum Chromodynamics and the Deep Structure of Elementary Particles”, contract FMRX-CT98-0194 (DG 12-MIHT).

The key role played by the vector mesons in the dynamics of hadron photoproduction on nucleons, at energies sufficiently above the vector-meson production thresholds, became clear in the late sixties and early seventies. Indeed, the total photoproduction cross-section on protons,  $\sigma_{\gamma p}(W^2)$ , was found to be related to forward vector-meson photoproduction,  $d\sigma^0/dt|_{\gamma p \rightarrow V p}(W^2)$ , extrapolated to  $t = 0$  [1]<sup>1</sup>,

$$\sigma_{\gamma p}(W^2) = \sum_{V=\rho^0, \omega, \phi, J/\psi} \sqrt{16\pi} \sqrt{\frac{\alpha\pi}{\gamma_V^2}} \left( \frac{d\sigma^0}{dt} \Big|_{\gamma p \rightarrow V p}(W^2) \right)^{1/2}, \quad (1)$$

and to the total cross-sections for the scattering of transversely polarized vector mesons on protons,  $\sigma_{V p}$ , obtained [2] by applying the additive quark model for hadron–hadron interactions

$$\sigma_{\gamma p}(W^2) = \sum_{V=\rho^0, \omega, \phi, J/\psi} \frac{\alpha\pi}{\gamma_V^2} \sigma_{V p}(W^2). \quad (2)$$

The factor  $\alpha\pi/\gamma_V^2$  in (1) and (2) denotes the strength of the coupling of the (virtual) photon to the vector meson  $V$ , as measured in  $e^+e^-$  annihilation by the integral over the vector-meson peak:

$$\frac{\alpha\pi}{\gamma_V^2} = \frac{1}{4\pi^2\alpha} \sum_F \int \sigma_{e^+e^- \rightarrow V \rightarrow F}(s) ds, \quad (3)$$

or by the partial width of the vector meson:

$$\Gamma_{V \rightarrow e^+e^-} = \frac{\alpha^2 m_V}{12(\gamma_V^2/4\pi)}. \quad (4)$$

The sum rules (1) and (2) are based on

- i) the direct couplings of the vector mesons to the photon and on
- ii) subsequent strong-interaction diffractive scattering of the vector mesons on the proton.

Relations (1) and (2) accordingly provide the theoretical basis for applying concepts of strong-interaction physics, such as Regge-pole phenomenology, to the interaction of the photon with nucleons. Compare [3] for a recent analysis of the experimental data for the total photoproduction cross-section in terms of Regge phenomenology.

The sum rule (1) is an approximate one. The fractional contributions of the different vector mesons to the total cross-section,  $\sigma_{\gamma p}$ , were found to be [4]<sup>2</sup>

$$r_\rho = 0.65, \quad r_\omega = 0.08, \quad r_\phi = 0.05, \quad (5)$$

---

<sup>1</sup>A precision evaluation of (1) requires a correction for the (small) ratio of real to imaginary forward scattering amplitudes to be inserted in the right-hand side of (1).

<sup>2</sup>Compare also the review [5].

adding up to approximately 78 % of the total cross-section. An additional contribution of  $r_{J/\psi} \simeq 1\text{--}2\%$  has to be added for the  $J/\psi$  vector meson. To saturate the sum rule (1), the contributions of the leading vector mesons have to be supplemented by more massive contributions also coupled to the photon, as observed in  $e^+e^-$  annihilation. From the point of view of generalized vector dominance (GVD) [4], the sum rules (1) and (2) appear as an approximation that is reasonable for the  $Q^2 = 0$  case of photoproduction, while breaking down with increasing space-like  $Q^2$ , the role of  $\rho^0$ ,  $\omega$  and  $\phi$  being taken over by more massive states.

Relations (1) and (2) implicitly contain the propagators of the different vector mesons. Being evaluated for real photons at  $Q^2 = 0$ , no explicit propagator factors appear in (1) and (2), and the photon vector-meson transition with subsequent vector-meson propagation is reduced to a multiplication of the various cross-sections by coupling constants characteristic of the vector-meson photon junctions. It was pointed out a long time ago [6]<sup>3</sup> that an experimental study of vector-meson electroproduction would provide an additional and particularly significant test of the underlying photoproduction dynamics.

The presence of the vector-meson propagators in the respective production amplitudes for the various vector mesons would be explicitly tested in vector-meson electroproduction. In addition, vector-meson production by virtual photons, at values of  $Q^2 \gg m_V^2$ , would allow to test the expected dominance of the production by longitudinal photons over the production by transverse ones. Moreover, the hypothesis of helicity conservation with respect to the centre-of-mass frame of the reaction  $\gamma^*p \rightarrow Vp$ , the hypothesis of ‘*s*-channel helicity conservation’ (SCHC), introduced in [6] by generalizing experimental results from photoproduction [8] to electroproduction, would become subject to experimental tests.

More recently, it was conjectured [9]–[14] that vector-meson electroproduction at large values of  $Q^2$  was calculable in perturbative QCD (pQCD) and would provide experimental tests of it. We will comment on the results from the pQCD approach below.

Expressing the cross-section for forward ( $t \simeq 0$ ) production of vector mesons on nucleons by transversely polarized virtual photons in terms of the respective real-photon cross-sections, we have the vector-meson dominance model (VDM) prediction [6]

$$\frac{d\sigma_T^0}{dt}|_{\gamma^*p \rightarrow Vp}(W^2, Q^2) = \frac{m_V^4}{(Q^2 + m_V^2)^2} \frac{d\sigma^0}{dt}|_{\gamma p \rightarrow Vp}(W^2). \quad (6)$$

For longitudinally polarized virtual photons, as a consequence of the coupling of the vector meson  $V$  to a conserved source as required by electromagnetic current

---

<sup>3</sup>See also [7].

conservation, the result [6]

$$\frac{d\sigma_L^0}{dt}|_{\gamma^* p \rightarrow V p}(W^2, Q^2) = \frac{m_V^4}{(Q^2 + m_V^2)^2} \xi_V^2 \frac{Q^2}{m_V^2} \frac{d\sigma^0}{dt}|_{\gamma p \rightarrow V p}(W^2) \quad (7)$$

was obtained. Both relations (6) and (7) contain SCHC. The parameter  $\xi_V$  denotes the ratio of the imaginary forward scattering amplitudes for the scattering of longitudinally and transversely polarized vector mesons and may in principle depend on the vector meson  $V$  under consideration and on the energy  $W$ . The value of  $\xi_V = 1$  corresponds to the conjecture of helicity independence of vector-meson nucleon scattering in the high-energy limit.

The predictions (6) and (7) for vector-meson production by virtual photons are based on the idealization that the propagation of the single vector meson  $V$  is responsible for the  $Q^2$  dependence of the diffractive electroproduction of that vector meson  $V$ . This idealization is by no means true in nature. Time-like photons also couple to the continuum of hadronic states beyond  $\rho^0$ ,  $\omega$ ,  $\phi$ , etc., resulting from  $e^+e^-$  annihilation into quark-antiquark pairs, and vector-meson forward scattering need not necessarily be ‘diagonal’ in the masses of the ingoing and outgoing vector mesons. The process of diffraction dissociation, corresponding in the present context to ‘off-diagonal’ transitions such as  $\rho^0 p \rightarrow \rho'^0 p$  etc., is in fact well known to exist in hadron-hadron interactions, as explicitly observed in proton-proton scattering [15].

The modification of the vector-meson electroproduction cross-section resulting from the inclusion of off-diagonal transitions of the diffraction-dissociation type was investigated in [16]. For definiteness, in [16], the calculation of vector-meson production was based on a spectrum of an infinite series of vector-meson states coupled to the photon in a manner that assures duality to quark-antiquark production in  $e^+e^-$  annihilation. Under the fairly general assumption of a power law for the diffraction-dissociation amplitudes (at zero  $t$ ) in terms of the ratios of the masses of the diffractively produced vector states

$$T[V p \rightarrow V_N p] = c_0 T[V p \rightarrow V p] \left( \frac{m_1}{m_N} \right)^{2p+1} \quad (N = 1, 2, 3, \dots), \quad (8)$$

an intuitively very simple and satisfactory result was obtained.

The sum of the poles in the transverse amplitude for  $\gamma^* p \rightarrow V p$  was shown to sum up approximately to a single pole, the pole mass  $m_V$  of the vector meson  $V$  being changed, however, to a value of  $m_{V,T}$  different from  $m_V$ . Prediction (6), taking into account off-diagonal transitions as embodied in GVD, thus becomes [16]<sup>4</sup>

$$\frac{d\sigma_T^0}{dt}|_{\gamma^* p \rightarrow V p}(W^2, Q^2) = \frac{m_{V,T}^4}{(Q^2 + m_{V,T}^2)^2} \frac{d\sigma_T^0}{dt}|_{\gamma p \rightarrow V p}(W^2). \quad (9)$$

---

<sup>4</sup>The simple result (9) is an approximation that coincides with the full GVD result at  $Q^2 = 0$  and  $Q^2 \rightarrow \infty$ , but may vary by  $\sim 10\%$  at intermediate  $Q^2$  values.

For destructive interference among neighbouring vector-meson states, incorporated in [16] through an alternating-sign series of vector-meson states, one finds

$$m_{V,T} < m_V . \quad (10)$$

The alternating-sign assumption was originally motivated by GVD investigations of the total virtual photo-absorption cross-section [17]. (For a recent analysis see e.g. [18]). Alternating signs appear also in a recent QCD analysis [14] of  $\rho$ ,  $\rho'$ , and  $\rho''$  diffractive photo- and electroproduction. The precise value of  $m_{V,T}$  in (9) depends on the details of the strong amplitude, i.e. on the strength  $c_0$  and the exponent  $p$  of the power-law ansatz (8) for (spin-conserving) diffraction dissociation.

With (9), the asymptotic behaviour of the transverse forward-production cross-section in (off-diagonal) GVD becomes

$$\frac{d\sigma_T^0}{dt}|_{\gamma^* p \rightarrow Vp}(W^2, Q^2 \rightarrow \infty) = \frac{m_{V,T}^4}{Q^4} \frac{d\sigma^0}{dt}|_{\gamma p \rightarrow Vp}(W^2) . \quad (11)$$

While the power of  $Q^2$  in (9) and (11) remains unchanged with respect to (6), the normalization of the asymptotic cross-section relative to photoproduction is affected by the fourth power of  $m_{V,T}$ . Concerning sum rule (1): it is unaffected by the introduction of off-diagonal terms, since the initial photon remains, when passing from the left-hand side to right-hand side of (1). In relation (2), off-diagonal terms with destructively interfering amplitudes imply multiplication of each  $\sigma_{Vp}$  by a specific correction factor somewhat smaller than unity [16].

The result (9) (or rather the underlying amplitude) with the constraint (10) in [16] was obtained by straightforward summation of an alternating series. In view of the ensuing extension to longitudinal photons, we note that the transverse amplitude may, to a good approximation, be represented by a sum of dipole terms<sup>5</sup> by combining neighbouring terms in the series. Switching to an equivalent continuum formulation, we obtain the following representation of the transverse amplitude as an integral over dipoles

$$A_{T,\gamma^* p \rightarrow Vp}(W^2, Q^2, t = 0) = m_{V,T}^2 \int_{m_{V,T}^2} \frac{dm^2}{(Q^2 + m^2)^2} A_{\gamma p \rightarrow Vp}(W^2, t = 0) . \quad (12)$$

Note that the modified pole mass  $m_{V,T}$  of the discrete formulation has turned into an effective threshold in (12). Upon integration and squaring we immediately recover (9).

We note that our simple ansatz for diffraction dissociation does not lead to the change of the  $W$  dependence of vector-meson production with increasing  $Q^2$  for

---

<sup>5</sup> Although always possible, given the result (9) of the series, the dipole approximation of two neighbouring terms in the series is most natural for the choice  $p = 0$  in (8), the value supported by diffraction-dissociation data [15].

which there is some experimental indication [19]. Such an effect can be incorporated into GVD by modifying the  $W$  dependence of diffraction dissociation. Any additional  $W$ -dependence in GVD is expected to enter via the ratio  $x \simeq Q^2/W^2$  and yield an additional (mild)  $Q^2$  dependence beyond the propagator effect.

The impact of off-diagonal transitions on the result for longitudinally polarized virtual photons (7) was not explored in [16]. The representation (12) for the transverse production amplitude as a continuous sum over dipole contributions, abstracted from the assumed destructive interference between production amplitudes from neighbouring states, is well suited for a generalization to longitudinal photons. Taking into account the coupling of the photon to a conserved source as transmitted to the hadronic amplitude, we have

$$A_{L,\gamma^*p \rightarrow Vp}(W^2, Q^2, t=0) = \xi_V m_{V,L}^2 \int_{m_{V,L}^2} \sqrt{\frac{Q^2}{m^2}} \frac{dm^2}{(Q^2 + m^2)^2} A_{\gamma p \rightarrow Vp}(W^2, t=0) . \quad (13)$$

In deriving (13), we have taken  $\xi_V$  to be  $m$ -independent. We expect the threshold mass of the longitudinal amplitude,  $m_{V,L}$ , to be larger than  $m_T$ , i.e.  $m_{V,T}^2 < m_{V,L}^2 < m_V^2$ . This is certainly true if the occurrence of an additional inverse mass, associated with the extra  $\sqrt{Q^2}$  factor in  $A_{L,\gamma^*p \rightarrow Vp}$ , is the only difference between the  $m$ -dependence of  $A_{T,\gamma^*p \rightarrow Vp}$  and  $A_{L,\gamma^*p \rightarrow Vp}$ . A priori, the transverse and longitudinal (strong-interaction) diffraction-dissociation amplitudes  $T_{T/L}[Vp \rightarrow V_Np]$  may possess different  $m$ -dependences ( $p_L \neq p_T$  in (8)), thus affecting the ratio  $m_{V,L}^2/m_{V,T}^2$ .

Integration of (13) yields

$$\begin{aligned} A_{L,\gamma^*p \rightarrow Vp}(W^2, Q^2, t=0) &= \quad (14) \\ &\xi_V \left[ \frac{\pi}{2} \frac{m_{V,L}^2}{Q^2} - \frac{m_{V,L}^3}{\sqrt{Q^2}(Q^2 + m_{V,L}^2)} - \frac{m_{V,L}^2}{Q^2} \arctan \frac{m_{V,L}}{\sqrt{Q^2}} \right] A_{\gamma p \rightarrow Vp}(W^2, t=0) \\ &\rightarrow \frac{2}{3} \xi_V \frac{\sqrt{Q^2}}{m_{V,L}} A_{\gamma p \rightarrow Vp}(W^2, t=0) \quad \text{for } Q^2 \rightarrow 0 \\ &\rightarrow \frac{\pi}{2} \xi_V \frac{m_{V,L}^2}{Q^2} A_{\gamma p \rightarrow Vp}(W^2, t=0) \quad \text{for } Q^2 \rightarrow \infty . \end{aligned}$$

The above predictions for transverse and longitudinal production amplitudes are valid for high-energy ( $x = Q^2/(W^2 + Q^2) \ll 1$ ) forward ( $t \simeq 0$ ) production. It would be preferable to compare the predictions with forward-production data, thus eliminating the influence of a possible  $Q^2$  dependence of the slope of the  $t$ -distribution. No reliable data for forward production have been extracted from the experiments so far. Accordingly, in order to be able to compare at all with data available at present, we ignore a possible  $Q^2$  dependence of the  $t$ -distribution by putting  $b(0)/b(Q^2) \simeq 1$ , where  $b$  is the slope parameter in the  $t$ -distribution,  $\exp(-b|t|)$ . From (9), the transverse production cross-section integrated over  $t$

then becomes

$$\sigma_{T,\gamma^* p \rightarrow V p}(W^2, Q^2) = \frac{m_{V,T}^4}{(Q^2 + m_{V,T}^2)^2} \sigma_{\gamma p \rightarrow V p}(W^2) . \quad (15)$$

A remark on SCHC is appropriate at this point. From photoproduction measurements at lower energies it is known [5] that SCHC is not strictly valid. It is violated (at non-zero  $t$ ) at the level of approximately 10%. In vector dominance this amount of helicity-flip contributions is traced back to helicity-flip contributions in diffractive hadron reactions which occur at approximately the same rate. It is natural, accordingly, that the diffractive scattering of vector states leading to (12) also violates SCHC at the level of 10%. Hence the ansatz (12) has to hold as well for the helicity-flip transitions occurring at finite  $t$ . The relative amount of helicity-flip contributions has to remain at the level of 10% found in photoproduction.

The same arguments on SCHC also hold for the longitudinal cross section, or rather the longitudinal-to-transverse ratio  $R_V$ . From (14) and (15) we obtain

$$\begin{aligned} R_V(W^2, Q^2) &= \frac{\sigma_{L,\gamma^* p \rightarrow V p}}{\sigma_{T,\gamma^* p \rightarrow V p}} \quad (16) \\ &= \frac{(Q^2 + m_{V,T}^2)^2}{m_{V,T}^4} \xi_V^2 \left[ \frac{\pi}{2} \frac{m_{V,L}^2}{Q^2} - \frac{m_{V,L}^3}{\sqrt{Q^2}(Q^2 + m_{V,L}^2)} - \frac{m_{V,L}^2}{Q^2} \arctan \frac{m_{V,L}}{\sqrt{Q^2}} \right]^2 \\ &\rightarrow \frac{4}{9} \xi_V^2 \frac{Q^2}{m_{V,L}^2} \quad \text{for } Q^2 \rightarrow 0 \\ &\rightarrow \frac{\pi^2}{4} \xi_V^2 \frac{m_{V,L}^4}{m_{V,T}^4} \quad \text{for } Q^2 \rightarrow \infty . \end{aligned}$$

The approach to the large- $Q^2$  limit is rather slow, but note the enhancement factor  $(m_{V,L}/m_{V,T})^4$  in (16). For completeness, we quote also the total virtual-photon cross-section and its asymptotic limit

$$\begin{aligned} \sigma_{\gamma^* p \rightarrow V p}(W^2, Q^2) &\equiv \sigma_{T,\gamma^* p \rightarrow V p} + \epsilon \sigma_{L,\gamma^* p \rightarrow V p} \\ &= \sigma_{T,\gamma^* p \rightarrow V p} \left( 1 + \epsilon R_V(W^2, Q^2) \right) \quad (17) \\ &\rightarrow \frac{m_{V,T}^4}{Q^4} \left( 1 + \epsilon \frac{\pi^2}{4} \xi_V^2 \frac{m_{V,L}^4}{m_{V,T}^4} \right) \sigma_{\gamma p \rightarrow V p}(W^2) \quad (Q^2 \rightarrow \infty) . \end{aligned}$$

In the comparison of our predictions with experiment, we proceed in two steps. In a first step we consider the experimental evidence for the validity of SCHC, before we turn to a comparison of (15)–(17) with HERA data<sup>6</sup>. The

<sup>6</sup>For the preprint we consider only the statistical errors of the preliminary data and postpone a systematic error analysis for the journal version until the final experimental results become available.

$W$ [GeV]	$Q^2$ [GeV $^2$ ]	$\frac{M(00)}{M(++)}$	$\frac{M(+0)}{M(++)}$	$\frac{M(+-)}{M(++)}$	$\frac{M(0+)}{M(00)}$	$\chi^2$ /d.o.f.
9.4	0	—	$0.14 \pm 0.02$	$-0.05 \pm 0.02$	—	—
40–100	3–5	1.57	0.081	0.05	0.03	2.3
	5–30	2.02	0.24	0.01	- 0.03	0.41
	3–30	1.77	0.15	0.04	- 0.001	1.8

Table 1: The ratios of the helicity amplitudes  $M(\lambda_\gamma, \lambda_\rho)$  for  $\gamma^* p \rightarrow \rho^0 p$  obtained from a fit to the  $\rho^0$  density matrix elements as measured at HERA [20]. Only the central results are quoted and the  $\chi^2$  values are based on merely the statistical errors (cf. footnote 6). The photoproduction results (first row) are from [5].

validity of SCHC is not only of much interest in itself, due to the presence of the longitudinal degree of freedom of the virtual photon in electroproduction, but is as well a prerequisite for the determination of  $R_V$ , as long as data are lacking for a direct separation of  $\sigma_{T,\gamma^* p \rightarrow V p}$  and  $\sigma_{L,\gamma^* p \rightarrow V p}$ .

A recent measurement by the ZEUS collaboration [20] of the full set of 15 density matrix elements determining the vector-meson ( $\rho^0$  and  $\phi$ ) decay distribution [21] can be analyzed in terms of helicity-conserving and helicity-flip amplitudes. Using parity invariance as well as natural-parity exchange, the number of independent helicity amplitudes determining the density matrix elements can be reduced to ten. This number is reduced to five, if nucleon helicity-flip amplitudes are assumed to vanish. The normalized density matrix elements, accordingly, depend on four ratios of amplitudes, if we take the amplitudes to be purely imaginary. In a fit to the  $\rho^0$  density matrix elements, we have determined these ratios<sup>7</sup>.

As the third column in table 1 shows, the production of longitudinal  $\rho^0$  mesons by longitudinal photons strongly dominates the production of transverse  $\rho^0$  mesons by transverse photons. The fourth column in table 1 shows that the helicity-flip amplitude for production of longitudinal  $\rho^0$  mesons by transverse photons is suppressed to a value of order 15% relative to the (sub-)dominant transverse helicity-conserving amplitude. This result is consistent of what is known from photoproduction and hadron–hadron interactions at lower energies [5]. Finally, the last two columns in table 1 show that the remaining helicity-flip amplitudes are small. Hence, the central predictions of vector dominance at large  $Q^2$ , the dominant role of longitudinal photons and helicity conservation to the extent characteristic for diffractive hadron–hadron scattering, are confirmed by the measurements.

We note that a one-parameter fit to the data, assuming SCHC, yields values

<sup>7</sup>Current data are not yet precise enough to include nucleon helicity-flip amplitudes in a (nine-parameter) fit to the density-matrix elements. Nevertheless, such a fit shows that our main conclusions remain unchanged: The values for  $R_V$  remain consistent with the ones obtained assuming SCHC, and (some) helicity-flip contributions are of the order of 15%.

of the longitudinal-to-transverse ratio  $M(00)/M(++)$  consistent with the values from the four-parameter fit, the  $\chi^2/\text{d.o.f.} \simeq 2.8, 2.0, 3.2$  for the three  $Q^2$  rows of table 1, respectively, being substantially worse, however. A small violation of SCHC is necessary indeed.

We finally note that the value for  $R_\rho$  obtained from table 1,  $R_\rho = \{|M(00)|^2 + 2|M(0+)|^2\}/\{|M(++)|^2 + |M(+0)|^2 + |M(+-)|^2\} \simeq |M(00)|^2/|M(++)|^2 \simeq 2.4$  (4.0) for  $3 < Q^2 < 5 \text{ GeV}^2$  ( $5 < Q^2 < 30 \text{ GeV}^2$ ) is consistent with the previous determination of  $R_\rho$  from ZEUS. For the previous determination, the results of which will be shown below, the validity of SCHC had to be assumed.

We now turn to the  $Q^2$  dependence and compare predictions (15)–(17) with experimental data from HERA [20, 22] at an average  $\gamma^*p$  c.m. energy of  $W = 80 \text{ GeV}$  (50 GeV) for  $\phi$  ( $\rho^0$ ) production<sup>8</sup>. For a given vector meson  $V$ , our predictions depend on four parameters, the two effective vector-meson masses  $m_{V,T}$  and  $m_{V,L}$ , the ratio  $\xi_V$  of the longitudinal-to-transverse strong-interaction amplitudes, and the photoproduction cross-section, i.e. (15) at  $Q^2 = 0$ . The solid lines in Figs. 1–3 show the result of a simultaneous four-parameter fit to the data for  $\sigma_{\gamma^*p \rightarrow Vp}$  and  $R_V$ , performed separately for the  $\rho^0$  and the  $\phi$  meson. The data are well described by the fits, with the parameters

$$\begin{aligned} \xi_\rho &= 1.06, & m_{\rho,T}^2 &= 0.68 m_\rho^2, & m_{\rho,L}^2 &= 0.71 m_\rho^2, \\ \xi_\phi &= 0.90, & m_{\phi,T}^2 &= 0.43 m_\phi^2, & m_{\phi,L}^2 &= 0.60 m_\phi^2, \end{aligned} \quad (18)$$

and  $\sigma_{\gamma p \rightarrow \rho p} = 11.1 \mu\text{b}$ ,  $\sigma_{\gamma p \rightarrow \phi p} = 1.2 \mu\text{b}$ . The statistical errors in the parameters are small compared with the estimated systematic ones<sup>6</sup>.

The quality of the fits strongly supports the underlying picture: the propagation of hadronic spin-1 states and destructive interference govern the  $Q^2$  dependence of exclusive electroproduction of vector mesons at small  $x$  and arbitrary  $Q^2$ . Both the asymptotic  $1/Q^4$  behaviour of the cross section, see (17), and the flattening of  $R_V$ , see (16), are clearly visible in the data. Moreover, the fitted values (18) are in accordance with theoretical expectation. The value of  $\xi_V \simeq 1$ , i.e. helicity independence of diffractive vector-meson scattering, is very gratifying indeed. The mass parameters,  $m_{V,T}$  and  $m_{V,L}$ , show the theoretically expected ordering  $m_{V,T}^2 < m_{V,L}^2 < m_V^2$ .

The values of  $R_V$  obtained in the fit seem somewhat low with respect to the central values of the data at large  $Q^2$ . This is of course merely a consequence of the fact that the large- $Q^2$   $R_V$  data hardly contribute to the overall  $\chi^2$ , owing to their large errors. Varying the four fit-parameters within one standard deviation from their best-fit values, we find that a considerable spread in  $R_V$  is allowed. In other words, with current data a precision determination of our parameters is not yet possible. In fact, a two-parameter fit results in a similar  $\chi^2$  (dashed lines in Figs. 1–3) as the four-parameter fit. In the two-parameter fit, obtained by fixing

---

<sup>8</sup> At HERA energies, we may take the polarization parameter  $\epsilon = 1$ .

$\xi_V = 1$  and  $m_{V,L}^2 = 1.5 m_{V,T}^2$  (corresponding to an asymptotic value  $R_V \rightarrow 5.5$ ), we find

$$m_{\rho,T}^2 = 0.62 m_\rho^2, \quad m_{\phi,T}^2 = 0.40 m_\phi^2, \quad (19)$$

and  $\sigma_{\gamma p \rightarrow \rho p} = 11 \mu\text{b}$ ,  $\sigma_{\gamma p \rightarrow \phi p} = 1.0 \mu\text{b}$ . With respect to the results of the fits given in (18) and (19), it may be worth quoting the estimate  $0.41 m_V^2 \lesssim m_{V,T}^2 \lesssim 0.74 m_V^2$  from [16], based on a reasonable choice of the diffraction-dissociation parameters in (8).

In Figs. 2b and 3b, we show the transverse cross-section,  $\sigma_{T,\gamma^* p \rightarrow V p}$ . The data in Figs. 2b and 3b were extracted from the data on  $\sigma_{\gamma^* p \rightarrow V p}$  in Fig. 1 with the help of our two-parameter fit<sup>9</sup> for  $R_V$ . Figures 2b and 3b demonstrate the dramatic difference at large  $Q^2$  between the data and the GVD prediction (15) with  $m_{V,T} < m_V$  on the one hand, and the VMD prediction (6), or rather (15) with  $m_{V,T} \equiv m_V$ , on the other hand.

Comparing the dotted VMD predictions in Figs. 2b and 3b for the transverse cross-section  $\sigma_{T,\gamma^* p \rightarrow V p}$  with the data for  $\sigma_{\gamma^* p \rightarrow V p}$  in Figs. 1a and 1b, one notices that the dotted curves would approximately describe the data for  $\sigma_{\gamma^* p \rightarrow V p} = \sigma_{T,\gamma^* p \rightarrow V p} + \sigma_{L,\gamma^* p \rightarrow V p}$ . This, at first sight paradoxical, coincidence of fits of  $\sigma_{T,\gamma^* p \rightarrow V p} + \sigma_{L,\gamma^* p \rightarrow V p}$ , entirely based on the transverse VMD formula, was in fact observed previously [19, 23, 24] in fits that vary the power of  $(Q^2 + m_V^2)$  at fixed mass  $m_V$ . Implicitly the fits obviously assume  $\sigma_{L,\gamma^* p \rightarrow V p} = 0$ , and, disregarding the information from vector-meson decay indeed seem to confirm  $\sigma_{L,\gamma^* p \rightarrow V p} = 0$ . This conclusion is inconsistent, however, with the results of the above analysis of the  $\rho^0$  density matrix elements. This analysis establishes beyond any doubt that longitudinal  $\rho^0$  mesons are almost exclusively produced by longitudinal (virtual) photons (compare table 1). The mentioned approximate coincidence of fits based on the VMD formula for  $\sigma_{T,\gamma^* p \rightarrow V p}$  with the data for  $\sigma_{T,\gamma^* p \rightarrow V p} + \sigma_{L,\gamma^* p \rightarrow V p}$  appears as a numerical accident.

Recent theoretical work on the electroproduction of vector mesons has been concentrated on attempts to deduce the cross-sections from perturbative [9]–[13] and non-perturbative [14] QCD. For the production cross-section by transversely polarized vector mesons, the calculations typically lead to a strong asymptotic decrease, as  $1/Q^8$ , modified sometimes by additional corrections to become  $1/Q^7$ . It may be argued [11] that the region of  $Q^2 \lesssim 30 \text{ GeV}^2$  explored at present, in which experiments find a fall-off rather like  $1/Q^4$ , is not sufficiently asymptotic for pQCD to yield reliable results. Further experiments at still larger values of  $Q^2$  will clarify the issue.

As for the longitudinal-to-transverse ratio,  $R_V$ , pQCD calculations led to the same result of a linear rise in  $Q^2$  as the simple VDM predictions, compare (6) and (7). Such a linear rise is always obtained, if electromagnetic current conservation is the only source of the  $Q^2$  dependence of  $R_V$ . For large  $Q^2$ , this linear rise is in

---

<sup>9</sup>No other procedure to extract  $\sigma_{T,\gamma^* p \rightarrow V p}$  suggests itself, as the number of data points for  $R_V$  is very small, and the  $Q^2$  values for  $\sigma_{\gamma^* p \rightarrow V p}$  and  $R_V$  are not identical.

conflict with experimental results. A behaviour of the cross-section for  $Q^2 \gg m_\rho^2$ , for both the production of longitudinally as well as transversely polarized  $\rho^0$  mesons, somewhat closer to the experimental data, was obtained in [12]; the calculation was based on open  $q\bar{q}$  production and parton-hadron duality. It is interesting to note that the resulting cross-sections have a VDM form<sup>10</sup> multiplied by correction factors depending on the scaling variable  $x$ . The asymptotic form for  $R_V$  derived in [12] has recently been reproduced in a calculation based on  $\rho^0$ -meson wave-functions [13]. In [13], also pQCD calculations of the helicity-flip amplitudes have been presented. While the general trend of the helicity-flip amplitudes is correctly reproduced, a detailed comparison shows that the  $\chi^2$  of these predictions is  $\chi^2 \simeq 44$ , i.e.  $\chi^2$  is not better than for a representation of the density matrix elements under the assumption of SCHC (with a value of  $\chi^2 \simeq 45$ ) as given above. The coincidence of the relative magnitude of the helicity-flip amplitudes at large  $Q^2$  with the helicity-flip amplitudes in photoproduction and diffractive hadron physics remains unexplained in the pQCD approach.

In summary, we have investigated electroproduction of vector mesons in GVD. We have shown that destructive interference between neighbouring vector states naturally leads to the spectral representations (12) and (13) of the (zero- $t$ ) amplitudes for  $\gamma_{T,L}^* + p \rightarrow V_{T,L} + p$ . Both predictions, the asymptotic  $1/Q^2$  fall-off of the transverse amplitude and the approach of  $R_V$  towards a constant value, are in good agreement with the experimental data. The expected hierarchy,  $m_{V,T}^2 < m_{V,L}^2 < m_V^2$ , of the pole masses  $m_{V,T}$ ,  $m_{V,L}$  and the helicity independence of the strong-interaction amplitudes (reflected in  $\xi_V \simeq 1$ ) strongly support the GVD picture: the propagation of hadronic vector states determines, for arbitrary  $Q^2$ , the  $Q^2$  dependence of vector-meson production by virtual photons in the diffraction region of  $x \simeq Q^2/W^2 \ll 1$ . Moreover as expected in this picture, SCHC is experimentally violated at the order of magnitude of 10%, the value typical for diffractive hadron-hadron scattering and photoproduction.

Returning to our starting point, the photoproduction sum rules (1) and (2), the present analysis strengthens their dynamical content, which is to reduce photoproduction to vector-meson-induced reactions. More generally, in conjunction with the experimental observation of states with masses up to about 20 GeV [25] in diffractive production in DIS at small  $x$  and up to large  $Q^2$ , the present investigation supports the point of view [26] that propagation and diffractive scattering of hadronic vector states is the basic dynamical mechanism in DIS at small values of the scaling variable.

#### *Acknowledgement*

It is a pleasure to thank Teresa Monteiro and Günter Wolf for useful discussions on the HERA data.

---

<sup>10</sup>Compare (37) and (38) in [12].

## References

- [1] L. Stodolsky, *Phys. Rev. Lett.* **18** (1967) 135.
- [2] H. Joos, *Phys. Lett.* **B24** (1967) 103;  
K. Kajantie and J.S. Trefil, *Phys. Lett.* **B24** (1967) 106;  
P.G.O. Freund, *Nuovo Cimento* **44A** (1966) 411.
- [3] A. Donnachie and P.V. Landshoff, *Phys. Lett.* **B296** (1992) 227;  
C. Caso et al., Particle Data Group, Review of Particle Properties, *Eur. Phys. J.*, **C3** (1998) 1.
- [4] J.J. Sakurai and D. Schildknecht, *Phys. Lett.* **40B** (1972) 121;  
B. Gorczyca and D. Schildknecht, *Phys. Lett.* **47B** (1973) 71.
- [5] D. Leith, in *Electromagnetic Interactions of Hadrons*, Plenum Press, New York, 1978, eds. A. Donnachie and G. Shaw, Vol. 1, p. 345.
- [6] H. Fraas and D. Schildknecht, *Nucl. Phys.* **B14** (1969) 543.
- [7] C.F. Cho and G.J. Gounaris, *Phys. Rev.* **186** (1969) 1619.
- [8] Aachen–Berlin–Bonn–Heidelberg–München collaboration, *Phys. Rev.* **175** (1968) 1669;  
W.G. Jones et al., *Phys. Rev. Lett.* **21** (1968) 586.
- [9] M.G. Ryskin, *Z. Phys.* **C57** (1993) 89.
- [10] S.J. Brodsky, L. Frankfurt, J.F. Gunion, A.H. Mueller and M. Strikman, *Phys. Rev.* **D50** (1994) 3134.
- [11] J.R. Cudell and I. Royon *Phys. Lett.* **B397** (1997) 317.
- [12] A.D. Martin, M.G. Ryskin and T. Teubner, *Phys. Rev.* **D55** (1997) 4329.
- [13] D.Yu. Ivanov and R. Kirschner, hep-ph/9807324.
- [14] H.G. Dosch, T. Gousset, G. Kulzinger and H.J. Pirner, *Phys. Rev.* **D55** (1997) 2602;  
G. Kulzinger, H.G. Dosch and H.J. Pirner, hep-ph/9806352.
- [15] K. Goulianos, *Phys. Rep.* **101** (1983) 169.
- [16] H. Fraas, B.J. Read and D. Schildknecht, *Nucl. Phys.* **B88** (1975) 301.
- [17] H. Fraas, B.J. Read and D. Schildknecht, *Nucl. Phys.* **B86** (1975) 346.
- [18] L. Frankfurt, V. Guzey and M. Strikman, hep-ph/9712339.

- [19] T. Monteiro for the ZEUS collaboration, in Proc. *5th Int. Workshop on Deep Inelastic Scattering and QCD*, Chicago, eds. J. Repond and D. Krakauer (American Institute of Physics, New York, 1997), p. 626.
- [20] ZEUS collaboration, papers submitted to XXIX Int. Conf. on High-Energy Physics, Abstracts 792, 793 and Addendum, Vancouver, 1998.
- [21] K. Schilling and G. Wolf, *Nucl. Phys.* **B61** (1973) 381.
- [22] ZEUS collaboration, M. Derrick et al., *Phys. Lett.* **B377** (1996) 259; ZEUS collaboration, M. Derrick et al., *Phys. Lett.* **B380** (1996) 220; H1 collaboration, C. Adloff et al., *Z. Phys.* **C75** (1997) 607. ZEUS collaboration, J. Breitweg et al., *Eur. Phys. J.* **C2** (1998) 247; ZEUS collaboration, J. Breitweg et al., DESY-98-107, 1998.
- [23] F. Gade for the H1 collaboration, in same Proc. as [19], p. 631.
- [24] M. Erdmann, plenary talk at the XXIX Int. Conf. on High Energy Physics, Vancouver, 1998.
- [25] H1 collaboration, T. Ahmed et al., *Nucl. Phys.* **B429** (1993) 477; ZEUS collaboration, M. Derrick et al., *Phys. Lett.* **B315** (1993) 481.
- [26] D. Schildknecht and H. Spiesberger, hep-ph/9707447; D. Schildknecht, *Acta Phys. Pol.*, **B28** (1997) 2453; D. Schildknecht, hep-ph/9806353, to appear in Proc. XXXIIrd Rencontres de Moriond, Les Arcs, 1998.

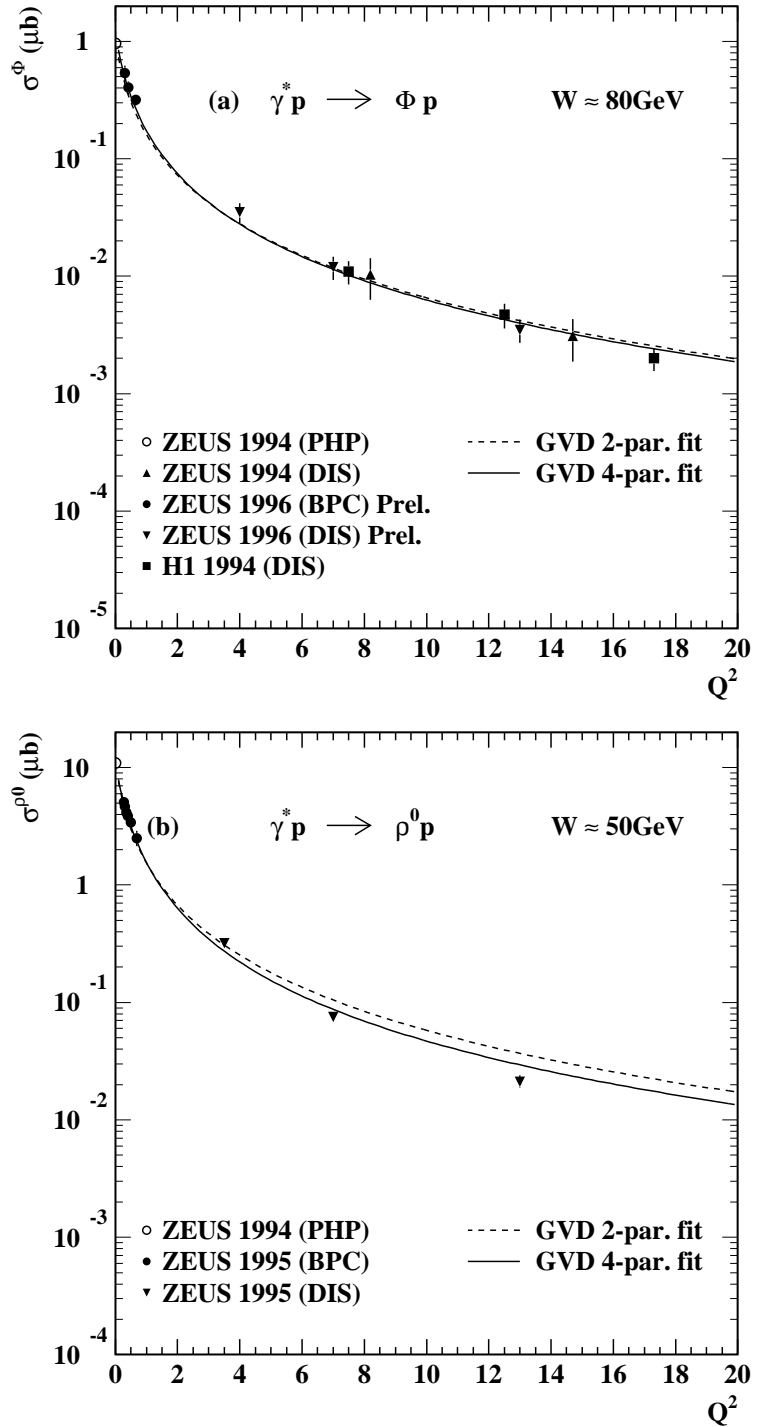


Figure 1: Data for  $\sigma_{\gamma^* p \rightarrow \phi p}$  (in (a)) and for  $\sigma_{\gamma^* p \rightarrow \rho p}$  (in (b)) from HERA compared with the GVD prediction (17). Solid lines: Four-parameter fit with the values (18) of the fit parameters. Dashed line: Two-parameter fit with the values (19) of the fit parameters.

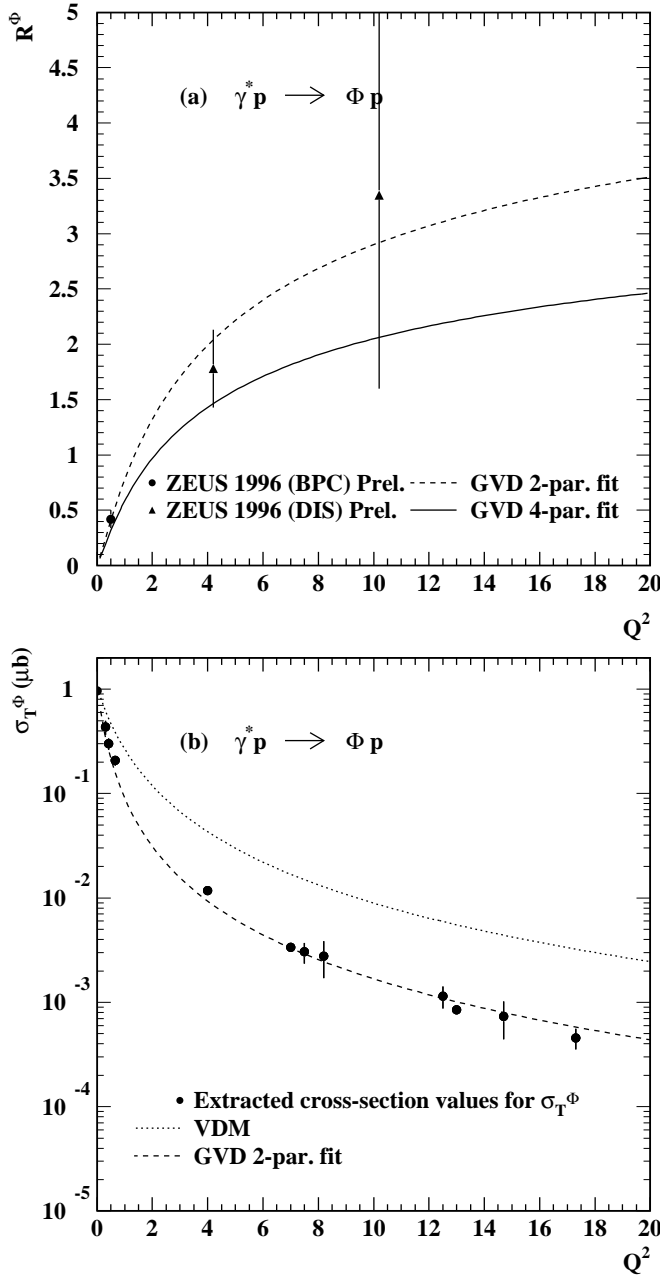


Figure 2: (a) HERA data for the longitudinal-to-transverse ratio  $R_\phi$  for  $\phi$  production extracted from the  $\phi$  decay distribution using SCHC, compared with the GVD prediction (16). Solid line: Four-parameter fit with the values (18) of the fit parameters. Dashed line: Two-parameter fit with the values (19) of the fit parameters.

(b) Data for  $\phi$  production by transversely polarized photons,  $\sigma_{T,\gamma^* p \rightarrow \phi p}$ , extracted from the measured values of  $\sigma_{\gamma^* p \rightarrow \phi p}$  by using the two-parameter  $R_\phi$  fit shown in (a). Dashed line: GVD prediction (15) with the two-parameter fit values (19). Dotted line: VDM prediction, i.e. (15) with  $m_{\phi,T} \equiv m_\phi$ .

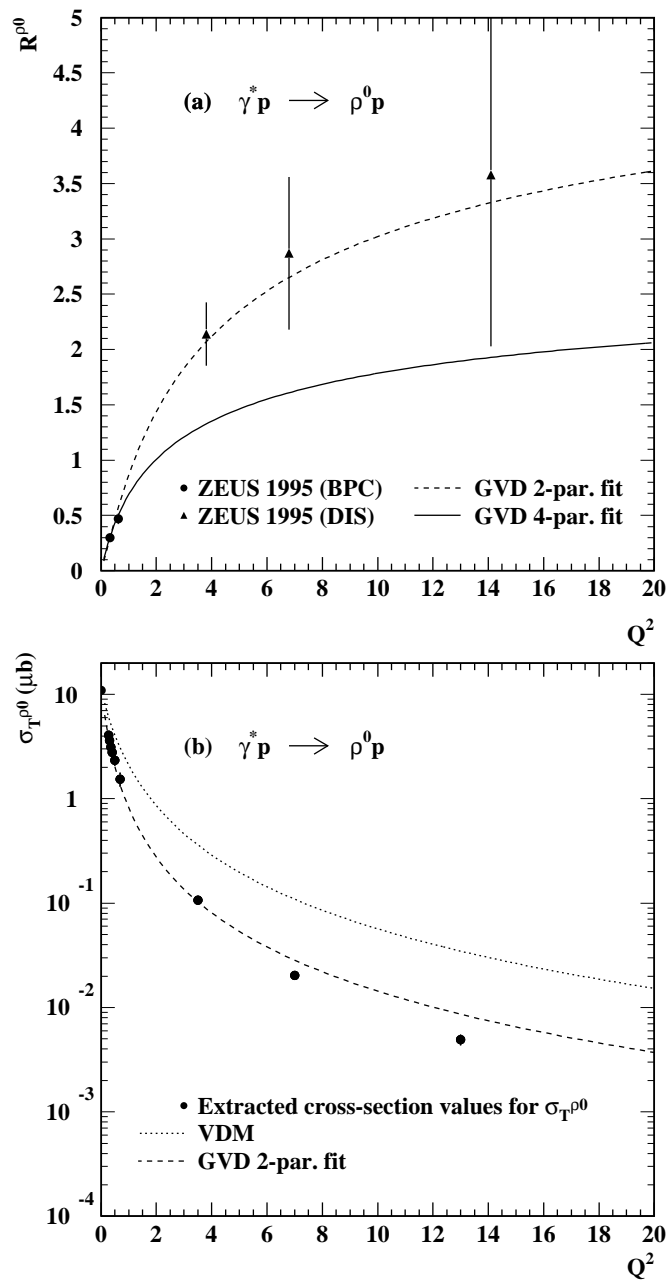


Figure 3: As Fig. 2, but for  $\rho^0$ -meson production.